The Astrophysical Journal Letters, 721:L158–L162, 2010 October 1 doi:10.1088/2041-8205/721/2/L158


# ACCURATE MASSES FOR THE PRIMARY AND SECONDARY IN THE ECLIPSING WHITE DWARF BINARY NLTT 11748*

Mukremin Kilic[1,4], Carlos Allende Prieto[2], Warren R. Brown[1], M. A. Agüeros[3], S. J. Kenyon[1], and Fernando Camilo[3]
[1] Smithsonian Astrophysical Observatory, 60 Garden St., Cambridge, MA 02138, USA; mkilic@cfa.harvard.edu
[2] Instituto de Astrofísica de Canarias, 38205 La Laguna, Tenerife, Spain
[3] Department of Astronomy, Columbia University, 550 West 120th Street, New York, NY 10027, USA
*Received 2010 May 21; accepted 2010 August 5; published 2010 September 13*

## ABSTRACT

We measure the radial velocity curve of the eclipsing detached white dwarf binary NLTT 11748. The primary exhibits velocity variations with a semi-amplitude of 273 km s$^{-1}$ and an orbital period of 5.641 hr. We do not detect any spectral features from the secondary star or any spectral changes during the secondary eclipse. We use our composite spectrum to constrain the temperature and surface gravity of the primary to be $T_{\rm eff} = 8690\pm140$ K and $\log g = 6.54 \pm 0.05$, which correspond to a mass of 0.18 $M_{\odot}$. For an inclination angle of 89.°9 derived from the eclipse modeling, the mass function requires a 0.76 $M_{\odot}$ companion. The merger time for the system is 7.2 Gyr. However, due to the extreme mass ratio of 0.24, the binary will most likely create an AM CVn system instead of a merger.

*Key words:* stars: individual (NLTT 11748) – stars: low-mass – white dwarfs

*Online-only material:* color figures

## 1. INTRODUCTION

Radial velocity observations of extremely low-mass white dwarfs (ELM WDs, 0.2 $M_{\odot}$) show that the majority are in close binaries. This is expected, as the Galaxy is not old enough to produce such WDs through single star evolution. Recent discoveries of seven short-period binary WDs that contain ELM WDs increased interest in these systems (Kilic et al. 2007, 2009, 2010; Vennes et al. 2009; Mullally et al. 2009; Marsh et al. 2010; Kulkarni & van Kerkwijk 2010). Five of these systems will merge within a Hubble time, with the merger time being shorter than 500 Myr for three of them. The extreme mass ratios of the binary components mean that some of these systems may not merge. Instead, they may be the long-sought progenitors of AM CVn stars. On the other hand, depending on the inclination angle and the true mass ratio, they may merge and create extreme helium stars, including R Coronea Borealis stars or single helium-enriched subdwarf O stars. If the mass transfer is dynamically unstable, an underluminous Type Ia supernova is also a possibility (Guillochon et al. 2010).

Kawka & Vennes (2009) report the discovery of a nearby ELM WD in the New Luyten catalog of stars with proper motions Larger than Two Tenths of an arcsecond (NLTT). Based on low-resolution spectroscopy, they find that NLTT 11748 has $T_{\rm eff} = 8540$ K, $\log g = 6.2$, and $M = 0.167\ M_{\odot}$. They estimate a distance of 199 pc. With a proper motion of 296.4 mas yr$^{-1}$ (Lépine & Shara 2005), NLTT 11748 has a tangential velocity of 280 km s$^{-1}$. If NLTT 11748 were a single star, its kinematic properties would be similar to the runaway WD LP400−22 (Kilic et al. 2009; Vennes et al. 2009; Kawka et al. 2006).

To search for a binary companion, we obtained optical spectroscopy observations of NLTT 11748 in 2009 September. Subsequently, Steinfadt et al. (2010) reported the discovery of 3%–6% eclipses in the $g$-band light curve of this star and Kawka et al. (2010) presented an ephemeris and secondary mass function. We use our spectroscopy data to confirm the period, search for spectroscopic signatures of the secondary star during an eclipse, and also constrain the mass of the primary and secondary stars accurately. Our observations are discussed in Section 2; the nature of the primary and the secondary are discussed in Sections 3 and 4.

## 2. OBSERVATIONS

### 2.1. MMT Optical Spectroscopy

Kawka & Vennes (2009) reported the discovery of NLTT 11748 on 2009 September 17. We obtained 52 spectra of NLTT 11748 with the 6.5 MMT and the Blue Channel Spectrograph on UT 2009 September 26–28. We used a 1″ slit and the 832 line mm$^{-1}$ grating in second order to obtain spectra with a wavelength coverage of 3550–4500 Å, a resolving power of $R =$ 4300, and an exposure time of 450 s. We obtained all spectra at the parallactic angle and acquired comparison lamp exposures either before or after every science exposure. We checked the stability of the spectrograph by measuring the centroid of the Hg emission line at 4358.34 Å from street lights. Over three nights, we measured an average offset of $-1.2\pm0.3$ km s$^{-1}$. We flux calibrated the spectra using the spectrophotometric standard BD+28 4211 (Massey et al. 1988).

To measure heliocentric radial velocities, we use the cross-correlation package RVSAO (Kurtz & Mink 1998). We obtain preliminary velocities by cross-correlating the observations with bright WD templates of known velocity. However, greater velocity precision comes from cross-correlating the object with itself. Thus, we shift the individual spectra to rest frame and sum them together into a high signal-to-noise ratio template spectrum. Individual spectra have a signal-to-noise ratio of 30 in the continuum at 4000 Å; the composite spectrum has a signal-to-noise ratio of 200. Our final velocities come from cross-correlating the individual observations with this template and are presented in Table 1.

We also use the best-fit WD model spectrum (see Section 3) to measure radial velocities. The results are consistent within 5 km s$^{-1}$. The mean velocity difference between the analyses is $3.0 \pm 0.6$ km s$^{-1}$. Thus, the systematic errors in our

* Based on observations obtained at the MMT Observatory, a joint facility of the Smithsonian Institution and the University of Arizona.
[4] *Spitzer* Fellow.

**Table 1**
Radial Velocity Measurements for NLTT 11748

| HJD +2455100 | Heliocentric Radial Velocity (km s$^{-1}$) |
|---|---|
| 0.937114 | 350.0 ± 2.8 |
| 0.942508 | 329.5 ± 3.2 |
| 0.950136 | 280.4 ± 2.8 |
| 0.955842 | 246.0 ± 2.6 |
| 0.961885 | 205.9 ± 2.1 |
| 0.969501 | 148.0 ± 3.7 |
| 0.974895 | 110.5 ± 2.4 |
| 0.980289 | 71.7 ± 3.5 |
| 0.987975 | 13.9 ± 3.7 |
| 0.993369 | −15.0 ± 2.8 |
| 0.998763 | −46.6 ± 3.8 |
| 1.005962 | −79.5 ± 3.4 |
| 1.011345 | −90.3 ± 3.9 |
| 1.016739 | −116.8 ± 4.7 |
| 1.021345 | −150.9 ± 7.5 |
| 1.880303 | 336.5 ± 3.4 |
| 1.932877 | −6.2 ± 2.5 |
| 1.938271 | −47.5 ± 4.2 |
| 1.943746 | −79.0 ± 2.7 |
| 1.951455 | −113.0 ± 2.7 |
| 1.956849 | −124.9 ± 2.9 |
| 1.962243 | −136.4 ± 3.1 |
| 1.969477 | −153.3 ± 3.0 |
| 1.980265 | −134.9 ± 3.8 |
| 1.985694 | −127.7 ± 2.4 |
| 1.992939 | −113.9 ± 3.0 |
| 1.998333 | −92.4 ± 4.7 |
| 2.003716 | −60.2 ± 2.9 |
| 2.009110 | −18.4 ± 2.7 |
| 2.014909 | 6.9 ± 3.4 |
| 2.018740 | 44.1 ± 4.8 |
| 2.022919 | 78.9 ± 6.9 |
| 2.026403 | 99.5 ± 7.0 |
| 2.928187 | −116.3 ± 3.6 |
| 2.933581 | −101.4 ± 3.0 |
| 2.938975 | −74.1 ± 2.4 |
| 2.946615 | −40.6 ± 3.0 |
| 2.952009 | −9.4 ± 2.7 |
| 2.957391 | 40.3 ± 2.6 |
| 2.962785 | 71.4 ± 4.5 |
| 2.970274 | 111.1 ± 2.5 |
| 2.975656 | 148.4 ± 4.0 |
| 2.981050 | 203.9 ± 3.1 |
| 2.986444 | 247.0 ± 2.9 |
| 2.993898 | 276.2 ± 4.6 |
| 2.999292 | 300.1 ± 2.9 |
| 3.004686 | 348.6 ± 2.8 |
| 3.010069 | 368.6 ± 2.4 |
| 3.015416 | 381.3 ± 3.7 |
| 3.018484 | 390.1 ± 4.8 |
| 3.021551 | 382.1 ± 5.1 |
| 3.024618 | 410.6 ± 5.7 |

measurements are ≈3 km s$^{-1}$. This small uncertainty gives us confidence that the velocities in Table 1 are reliable.

### 2.2. Green Bank Telescope

Without prior knowledge of the photometric eclipses discovered in this system, we targeted it for a millisecond pulsar companion search using the Green Bank Telescope (GBT; see Agüeros et al. 2009a). We observed NLTT 11748 on 2010 February 7 for 1.4 hr at 350 MHz, which is where a pulsar with a typical spectral index of $\alpha = -1.6$ would be brightest, with the Green Bank Ultimate Pulsar Processing Instrument (GUPPI) backend.[5] The data reduction was similar to that described in Agüeros et al. (2009b). We used the standard search techniques implemented in the PRESTO software package (Ransom 2001). Because PRESTO assumes a constant apparent acceleration, we divided our GBT data into eight separate 644.25 s integrations, each representing ∼3% of an orbit, and conducted searches for pulsations separately in each of these partial observations. Not surprisingly (given the 3%–6% eclipses detected in the optical light curve), no convincing pulsar signal is detected in our data.

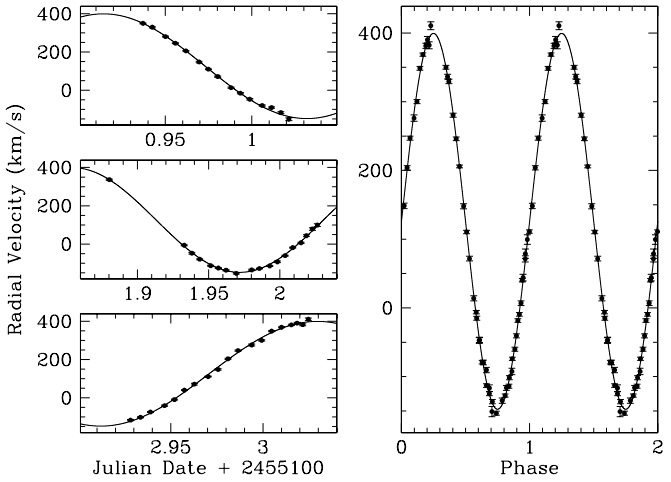


**Figure 1.** Radial velocity of NLTT 11748 (black dots) observed in 2009 September (left panels). The right panel shows all of these data points phased with the best-fit period. The solid line represents the best-fit model for a circular orbit with a radial velocity amplitude of 273.4 km s$^{-1}$ and a period of 0.23503 days.

## 3. RESULTS

The radial velocity of NLTT 11748 varies by as much as 564 km s$^{-1}$ between different observations, revealing the presence of a companion object. We compare the radial velocities of the H$\gamma$ and H$\delta$ lines with the H8 and higher order Balmer lines; there are no significant velocity differences between these lines. Hence, the observed Balmer lines are from only one star. We weight each velocity by its associated error and solve for the best-fit orbit using the code of Kenyon & Garcia (1986). We estimate the errors in the orbital parameters through Monte Carlo simulations of 10,000 sets of radial velocities. The heliocentric radial velocities are best fit with a circular orbit and a radial velocity amplitude $K = 273.4 \pm 0.5$ km s$^{-1}$. The best-fit orbital period is $0.23503 \pm 0.00013$ days (5.641 hr) with spectroscopic conjunction at HJD $2455100.855518 \pm 0.000069$. Based on the photometric light curve and eight separate spectra, Steinfadt et al. (2010) measure an orbital period of 0.2350606(11) days and a velocity semi-amplitude of 271 ± 3 km s$^{-1}$. In addition, Kawka et al. (2010) measure an orbital period of 0.235061(3) days and a velocity semi-amplitude of 274.8 ± 1.5 km s$^{-1}$. Our measurements are consistent with these estimates. Figure 1 shows the observed radial velocities and our best-fit period for NLTT 11748.

NLTT 11748 is near the Taurus–Auriga molecular cloud, and the 4430 Å diffuse interstellar band is detected in our high signal-to-noise ratio MMT spectrum (Figure 2). The observed

[5] http://wikio.nrao.edu/bin/view/CICADA/GUPPiUsersGuide

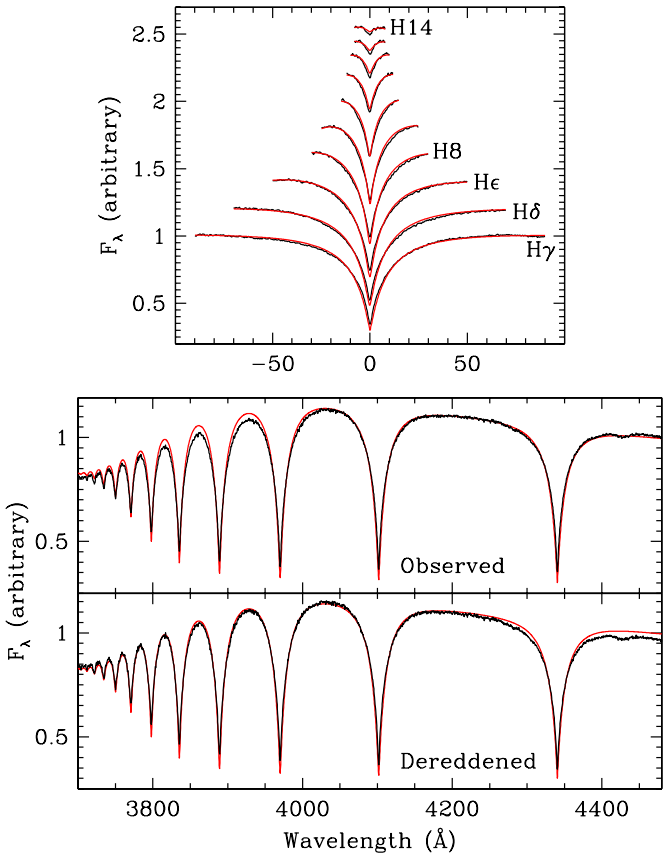


**Figure 2.** Spectral fits (solid lines) to the flux-normalized line profiles (jagged lines, top panel) and to the observed composite spectrum of NLTT 11748 (middle panel). The bottom panel shows the de-reddened spectrum.

(A color version of this figure is available in the online journal.)

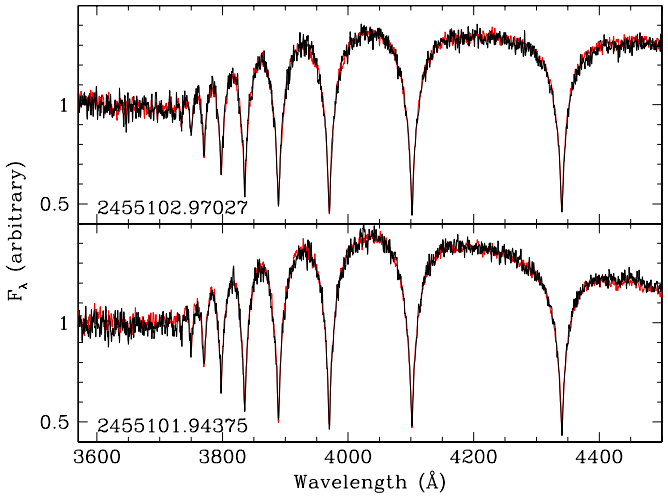


**Figure 3.** Secondary eclipse spectrum of NLTT 11748 (black line) compared to the average spectra taken immediately before and after the eclipse (red line). The top panel is for our ephemeris determination and the bottom panel is for the ephemeris found by Steinfadt et al. (2010). The mid-exposure HJD is given in each panel. No evidence of the companion is seen during secondary eclipse.

(A color version of this figure is available in the online journal.)

2%–3% absorption in this band corresponds to an extinction of $E(B-V) \approx 0.1$ (Krelowski et al. 1987), consistent with the Kawka & Vennes (2009) estimate.

We perform model fits to each individual spectrum and also to the composite spectrum using synthetic WD spectra kindly provided by D. Koester. We use the 52 individual spectra to obtain a robust estimate of the errors in our analysis. Figure 2 shows our model fits to the Balmer line profiles (top panel) and to the composite spectrum (middle panel). We obtain a best-fit solution of $T_{\rm eff} = 8690 \pm 140$ K and $\log g = 6.54 \pm 0.05$ from the observed composite spectrum. The best-fit model does not match the observed spectrum in the blue, especially the higher order Balmer lines (middle panel). Even in the fits to the observed line profiles (top panel), the lines remain poorly fit. The bottom panel in Figure 2 shows the de-reddened spectrum against this best-fit model. The line core strengths are overestimated in the models. This problem is not evident in the Kawka & Vennes (2009) analysis, which uses lower resolution and lower signal-to-noise ratio spectra limited to wavelengths longer than about 3800 Å.

Contribution from a cool companion could dilute the line profiles. We search for the spectral signature of such a companion using our spectroscopy during the secondary eclipse. Based on our orbital fit, one of the 52 spectra was obtained at phase 0 (see Figure 1) and it covers an entire 185 s secondary eclipse. Based on the orbital fit by Steinfadt et al. (2010), another one of our 52 spectra covers the secondary eclipse. We derive $T_{\rm eff} = 8620$ and 8490 K and $\log g = 6.53$ and 6.43 from these two spectra, respectively. These temperature and surface gravity estimates are consistent with $T_{\rm eff} = 8690 \pm 140$ K and $\log g = 6.54 \pm 0.05$ obtained from the composite spectrum. Figure 3 shows these two spectra compared to the average of the spectra taken immediately before and after the secondary eclipse. We do not detect significant differences between these spectra in either case, indicating that the secondary star does not significantly contribute to our spectrum. Hence, the observed line profiles cannot be explained by contribution from a binary companion.

Calibrating fluxes to better than a few percent over wavelength ranges spanning several hundred angstroms is a challenging task. Our flux calibration relies on the observations of the standard star BD+28 4211. Even though observations of the other targets from the same observing run do not show any flux calibration problems, NLTT 11748 is our brightest target and subtle systematic errors may be important. Comparing $T_{\rm eff} = 8690 \pm 140$ K and $\log g = 6.54 \pm 0.05$ from this study to the $T_{\rm eff} = 8540 \pm 50$ K and $\log g = 6.20 \pm 0.15$ from Kawka & Vennes (2009) shows excellent agreement between temperatures but a systematic offset in gravity. Differences in the fitting method employed (Kawka & Vennes used H$\alpha$ to H9 while the present study used H$\gamma$ to H14), model atmospheres, and flux calibration may all contribute toward a systematic offset between gravity measurements which are very sensitive to the strengths of the higher order Balmer lines. Fortunately, the differences in surface gravity do not significantly impact the mass derived from the mass–radius relations.

Figure 4 shows the effective temperature and surface gravity for NLTT 11748 (filled circle) along with the previously identified ELM WDs. Comparing our temperature and surface gravity measurements to Panei et al. (2007) models (updated by Kilic et al. 2010), NLTT 11748 has $M \approx 0.18\,M_{\odot}$. Using their best-fit model spectra and the mass–radius relation of Serenelli et al. (2002), Kawka & Vennes (2009) derive $M \approx 0.17\,M_{\odot}$, $M_V = 9.7 \pm 0.3$ mag, $d = 199 \pm 40$ pc (based on the Two Micron All Sky Survey $J$-band photometry), and a cooling age of 4–6 Gyr. Based on the updated Panei et al. (2007) models, NLTT 11748 has $M_V = 10.28$ mag, $R = 0.038\,R_{\odot}$, and $d = 152 \pm 30$ pc.

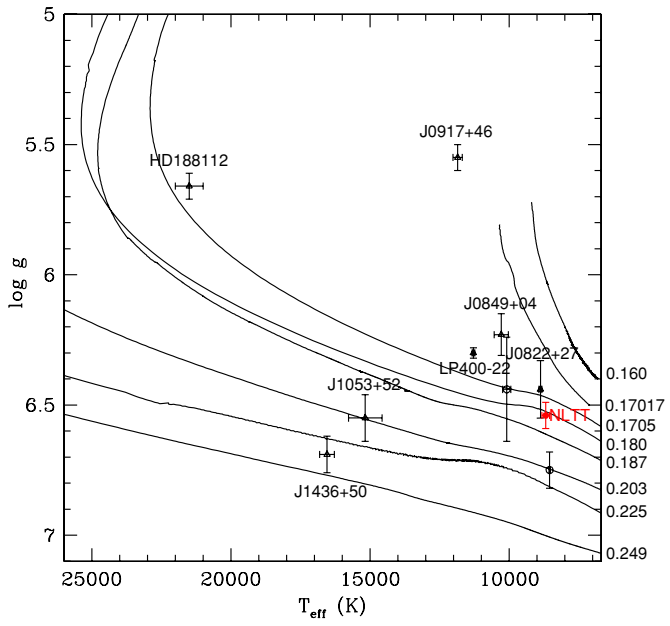


**Figure 4.** Best-fit solution for the surface gravity and temperature of NLTT 11748 (filled circle), overlaid on tracks of constant mass from Kilic et al. (2010, based on the Panei et al. 2007 models). Spectroscopically confirmed ELM WDs in the literature (see Kilic et al. 2010) and the subdwarf B star HD 188112 (Heber et al. 2003) are shown as open symbols.

(A color version of this figure is available in the online journal.)

The orbital period and the semi-amplitude of the radial velocity variations imply a mass function of $0.4978 \pm 0.0027$. For $M = 0.18\,M_{\odot}$ and the inclination angle of 89°.9 (Steinfadt et al. 2010), the companion is a $0.76\,M_{\odot}$ object at an orbital separation of $1.6\,R_{\odot}$.

## 4. DISCUSSION

Our radial velocity measurements show that NLTT 11748 is in a binary system with an orbital period of 5.641 hr. Our best-fit model cannot perfectly match the high-order Balmer line core strengths, however flux calibration is a possible culprit. Optical spectroscopy does not reveal any spectral features from a companion, and the observed 3%–6% eclipses in the light curve (Steinfadt et al. 2010) rule out main-sequence and neutron star companions. A relatively cold ($T_{\rm eff} \leqslant 7400$ K) $0.76\,M_{\odot}$ C/O WD is the only solution that satisfies the mass and radius constraints for the secondary star.

At a Galactic latitude of −28°.4, NLTT 11748 is 48 pc below the plane. The observed systemic velocity is $125.9 \pm 0.4$ (stat) $\pm 3.0$ (sys) km s$^{-1}$; the proper motion is $(\mu_{\alpha} \cos\delta, \mu_{\delta}) = (236.1, -179.2$ mas yr$^{-1}$; Lépine & Shara 2005). Our systemic velocity measurement is lower than that of Steinfadt et al. (2010) and Kawka et al. (2010) and the systematic errors dominate our velocity zero point. After correcting the systemic velocity for the gravitational redshift of 3 km s$^{-1}$, the velocity components with respect to the local standard of rest as defined by Hogg et al. (2005) are $U = -142 \pm 8, V = -187 \pm 41$, and $W = -29 \pm 6$ km s$^{-1}$. Clearly, NLTT 11748 is a halo star (see also Steinfadt et al. 2010; Kawka et al. 2010).

NLTT 11748 is the only known eclipsing detached double WD system. Modeling the optical light curve of the system, Steinfadt et al. (2010) derive a radius of ≈0.038–0.040 $R_{\odot}$ for a $0.18\,M_{\odot}$ primary WD. These estimates are entirely consistent with the Panei et al. (2007) model predictions of 0.038 $R_{\odot}$ for a 8690 K, $0.18\,M_{\odot}$ WD. This result provides the first test of the theoretical mass–radius relations for ELM WDs. The primary eclipse depth of 6.7% implies that the radius of the C/O WD is 26% of that of the ELM WD, i.e., 0.0099–0.0104 $R_{\odot}$. This range is entirely consistent with the theoretically predicted radii for $0.76\,M_{\odot}$ cool WDs (≈0.0105 $R_{\odot}$; Salaris et al. 2010).

The merger time due to loss of angular momentum through gravitational radiation is 7.2 Gyr. If the mass transfer is dynamically unstable, the system merges to produce an extreme helium star or an underluminous Type Ia supernova (Guillochon et al. 2010). However, with a mass ratio of 0.24, the mass transfer is probably stable (see Marsh et al. 2004; Nelemans et al. 2010, and references therein). NLTT 11748 is then one of the best known AM CVn progenitor candidates (see also Kilic et al. 2010).

## 5. CONCLUSIONS

Using high signal-to-noise ratio medium-resolution spectroscopy, we improve the mass estimates for the primary and secondary star in the eclipsing WD binary system NLTT 11748. We identify the visible component of the binary as a 8690 K, $0.18\,M_{\odot}$ WD at a distance of $152 \pm 30$ pc. The secondary is not detected in our MMT spectra. The mass function for the system requires a $0.76\,M_{\odot}$ C/O core WD companion. Taking all three available mass functions (0.480, 0.505, and 0.498) from Steinfadt et al. (2010), Kawka et al. (2010), and this study and two available spectroscopic mass estimates (0.17 and $0.18\,M_{\odot}$), we are confident that systematic errors do not influence our interpretation. The 3.5% deep secondary eclipses constrain the secondary to be relatively cool ($T_{\rm eff} \leqslant 7400$ K; Steinfadt et al. 2010). Follow-up time-series photometry to detect the secondary eclipses in several different filters will be useful to constrain the temperature and WD cooling age of the secondary star.

NLTT 11748 joins the growing list of short-period binary WDs including ELM WDs. Along with SDSS J0822+2753, J0849+0445, and J1257+5428 (Kilic et al. 2010; Marsh et al. 2010; Kulkarni & van Kerkwijk 2010), NLTT 11748 is likely to form an AM CVn system due to its extreme mass ratio.

We thank the referee S. Vennes for helpful suggestions, D. Koester for kindly providing WD model spectra, and S. Ransom for his help with the GBT observations. Support for this work was provided by NASA through the *Spitzer Space Telescope* Fellowship Program, under an award from Caltech. M.A.A. is supported by an NSF Astronomy and Astrophysics Postdoctoral Fellowship under award AST-0602099. The Robert C. Byrd Green Bank Telescope is operated by the National Radio Astronomy Observatory, which is a facility of the US National Science Foundation operated under cooperative agreement by Associated Universities, Inc.

*Facilities:* MMT (Blue Channel Spectrograph), GBT

## REFERENCES

Agüeros, M. A., Camilo, F., Silvestri, N. M., Kleinman, S. J., Anderson, S. F., & Liebert, J. W. 2009a, ApJ, 697, 283
Agüeros, M. A., et al. 2009b, ApJ, 700, L123
Guillochon, J., Dan, M., Ramirez-Ruiz, E., & Rosswog, S. 2010, ApJ, 709, L64
Heber, U., Edelmann, H., Lisker, T., & Napiwotzki, R. 2003, A&A, 411, L477
Hogg, D. W., Blanton, M. R., Roweis, S. T., & Johnston, K. V. 2005, ApJ, 629, 268
Kawka, A., & Vennes, S. 2009, A&A, 506, L25

Kawka, A., Vennes, S., Oswalt, T. D., Smith, J. A., & Silvestri, N. M. 2006, ApJ, 643, L123
Kawka, A., Vennes, S., & Vaccaro, T. R. 2010, A&A, 516, L7
Kenyon, S. J., & Garcia, M. R. 1986, AJ, 91, 125
Kilic, M., Brown, W. R., Allende Prieto, C., Kenyon, S. J., & Panei, J. A. 2010, ApJ, 716, 122
Kilic, M., Brown, W. R., Allende Prieto, C., Pinsonneault, M. H., & Kenyon, S. J. 2007, ApJ, 664, 1088
Kilic, M., Brown, W. R., Allende Prieto, C., Swift, B., Kenyon, S. J., Liebert, J., & Agüeros, M. A. 2009, ApJ, 695, L92
Krelowski, J., Walker, G. A. H., Grieve, G. R., & Hill, G. M. 1987, ApJ, 316, 449
Kulkarni, S. R., & van Kerkwijk, M. H. 2010, ApJ, 719, 1123
Kurtz, M. J., & Mink, D. J. 1998, PASP, 110, 934
Lépine, S., & Shara, M. M. 2005, AJ, 129, 1483
Marsh, T. R., Gaensicke, B. T., Steeghs, D., Southworth, J., Koester, D., Harris, V., & Merry, L. 2010, ApJ, submitted (arXiv:1002.4677)
Marsh, T. R., Nelemans, G., & Steeghs, D. 2004, MNRAS, 350, 113
Massey, P., Strobel, K., Barnes, J. V., & Anderson, E. 1988, ApJ, 328, 315
Mullally, F., Badenes, C., Thompson, S. E., & Lupton, R. 2009, ApJ, 707, L51
Nelemans, G., Yungelson, L. R., van der Sluys, M. V., & Tout, C. A. 2010, MNRAS, 401, 1347
Panei, J. A., Althaus, L. G., Chen, X., & Han, Z. 2007, MNRAS, 382, 779
Ransom, S. M. 2001, BAAS, 33, 1484
Salaris, M., Cassisi, S., Pietrinferni, A., Kowalski, P. M., & Isern, J. 2010, ApJ, 716, 1241
Serenelli, A. M., Althaus, L. G., Rohrmann, R. D., & Benvenuto, O. G. 2002, MNRAS, 337, 1091
Steinfadt, J. D. R., Kaplan, D. L., Shporer, A., Bildsten, L., & Howell, S. B. 2010, ApJ, 716, L146
Vennes, S., Kawka, A., Vaccaro, T. R., & Silvestri, N. M. 2009, A&A, 507, 1613